Proceedings of the ICBBG2025
2025 International conference on Bio-mediated and Bio-inspired Geotechnics
18-20 May, 2025 | Tempe, Arizona, USA
https://doi.org/10.53243/ICBBG2025-102

Integrating MICP with Geothermal Pavements: A Numerical Analysis of Thermal Performance and Cost-Efficiency

Xiaoying Gu, Ph.D.,[1] Alexandra Clarà Saracho, Ph.D.,[2] Nikolas Makasis, Ph.D.,[3] Monika Johanna Kreitmair, Ph.D.,[4] and Guillermo A. Narsilio Ph.D.[4]

[1]Department of Infrastructure Engineering, The University of Melbourne, Parkville, Australia, E-mail: annie.gu@unimelb.edu.au
[2]Department of Civil, Architectural and Environmental Engineering, The University of Texas at Austin, Austin, United States, E-mail: alexandra.clara.saracho@utexas.edu
[3]Department of Civil and Environmental Engineering, University of Surrey, Guildford, United Kingdom, E-mail: n.makasis@surrey.ac.uk
[4] Department of Civil and Environmental Engineering, University of Surrey, Guildford, United Kingdom, E-mail: m.kreitmair@surrey.ac.uk
[5] Department of Infrastructure Engineering, The University of Melbourne, Parkville, Australia, E-mail: narsilio@unimelb.edu.au

ABSTRACT

As demand for sustainable infrastructure grows, integrating microbial induced calcium carbonate precipitation (MICP) with geothermal pavements offers a promising way to enhancing energy efficiency and structural performance. This study investigates the technical and economic feasibility of MICP in geothermal pavement systems using a validated finite element model focused on a balanced thermal load case in Adelaide, South Australia. The thermal performance of MICP-treated geothermal pavements is evaluated under varying subbase saturation levels and subgrade thermal conductivities. Results show that MICP treatment significantly improves system performance in dry conditions (up to 70% increase in thermal output), especially when subgrade thermal conductivity is low (0.3 W/(m·K). However, effectiveness decreases when subbase saturation exceeds 10% or when subgrade thermal conductivity is high. Economically, feasibility depends heavily on MICP material costs. This study highlights the potential of MICP within a shallow geothermal context and emphasises the need to balance technical benefits with economic considerations.

INTRODUCTION

Rapid increases in global population are placing ever-growing demands on civil infrastructure, with the need for sustainable and energy-efficient solutions becoming increasingly pressing. One recent bio-geochemical method that has been widely researched is microbially induced calcium carbonate precipitation (MICP), due to its effectiveness in improving soil stability and its environmental friendliness (Li et al., 2020, Mujah et al., 2016). MICP utilises microorganisms to form calcium carbonate crystals ($CaCO_3$) that bridge air or water-filled pores between soil grains, enhancing the strength and stiffness of soils. MICP has been successfully used for several geotechnical applications, targeting soil strength improvement, erosion reduction, and liquefaction mitigation, amongst others (DeJong et al., 2010, Clarà Saracho et al., 2021, Mujah et al., 2016, Van Paassen, 2009). Moreover, MICP has been explored as a method for subbase stabilization of roads, offering a sustainable alternative to traditional cement-based stabilisers (Portugal et al., 2020, Xiao et al., 2022, Fu and Haigh, 2024).

In addition to the improvement of the mechanical properties of soils, MICP also has the potential for thermal enhancement. Several laboratory studies have already demonstrated the effectiveness of MICP in enhancing soil thermal conductivity (Zeinali et al., 2023, Xiao et al., 2021, Wang et al., 2020, Martinez et al., 2019, Venuleo et al., 2016). The $CaCO_3$ from MICP precipitates on particle contacts and surfaces, increasing the number of possible heat transfer paths. This significantly improves soil thermal conductivity, making MICP suitable for use with shallow geothermal systems. Shallow geothermal energy systems, also known as ground-source heat pump (GSHP) systems, utilise the relatively stable ground temperature via ground heat exchangers (GHEs) to provide heating and cooling, reducing reliance on conventional energy sources and decreasing carbon emissions. Geothermal pavements constitute one application of GHEs, integrated within pavement structures, enabling a secondary function in addition to structural stability (Gu et al., 2021, Arulrajah et al., 2021, del-Castillo-García et al., 2013). Soil thermal conductivity significantly impacts the cost-efficiency and performance of GHEs, as higher thermal conductivity facilitates more efficient heat transfer (Di Sipio and Bertermann, 2017, Kavanaugh, 2000).

Most studies of the application of MICP within roads have focused on utilising MICP to improve structural stability (Khosravi et al., 2024), with only limited exploration of its potential to enhance the thermal performance of geothermal pavements. Field-scale tests of MICP implementation face several challenges, including high costs and complex site requirements, the absence of uniform cost frameworks, and the difficulty of developing an optimal treatment method for uniform $CaCO_3$ formation (Rahman et al., 2020, Zhang et al., 2023). To address these challenges, numerical solutions such as finite element (FE) modelling offer a practical alternative. FE models have been widely employed to evaluate energy geostructures, providing reliable predictions of system performance under diverse conditions (Makasis and Narsilio, 2020, Insana and Barla, 2020, Zhong et al., 2022). These models can incorporate a range of parameters derived from laboratory tests, enabling comprehensive analysis of potential outcomes in field-scale applications.

This study uses an FE model, validated for a geothermal pavement system in Adelaide, South Australia (Gu et al., 2021), to assess the thermal potential and economic feasibility of a geothermal pavement system treated with MICP. Adelaide's relatively balanced heating and cooling demands are implemented to explore the ability of MICP to improve the performance of a geothermal system under a range of soil conditions. The analysis focuses on the system's thermal behaviour, assessing the effects of changing subbase thermal conductivity values and degrees of saturation. Additionally, an economic analysis is conducted to assess the financial feasibility of the system, comparing the additional capital cost of the MICP treatment with the energy savings achieved. This research aims to showcase how MICP can enhance geothermal pavement performance for balanced thermal load profiles, providing insights into the feasibility of this approach under local environmental conditions.

METHODOLOGY

This section introduces the validated FE model used to simulate the thermal performance of geothermal pavements with an MICP-treated subbase layer, which is typically composed of sand and serves as a cushion for the GHEs. The model is used to assess system performance under a relatively balanced thermal load condition, using Adelaide, as an example climate. Existing literature data is incorporated to evaluate the impact of MICP treatment on the pavement system under a range of conditions.

Finite Element Model.

This study adopts an experimentally validated FE model of geothermal pavements (Gu et al., 2021, Motamedi et al., 2021). This model incorporates the governing equations for fluid flow (momentum and continuity) and heat transfer (energy balance). Conductive heat transfer mainly occurs in the soil materials, including ground, structure backfills, and the HDPE pipe walls, while convective heat transfer is considered for the fluid flow inside the HDPE pipes. The energy balance equation is applied to simulate surface boundary conditions. Groundwater is not included in the model, due to the shallow depths considered. Details of the modelling equation and assumptions can be found in Gu et al. (2021).

Model Geometry and Parameters.

The meshed FE model and geometry of the designed geothermal pavement system is presented in Figure 1, along with the key boundary conditions. The GHEs are installed at 0.5 m below the pavement surface, with each circuit comprising 160.4 m of HDPE pipe. Each GHE circuit consists of 8 legs of HDPE pipes, spaced 0.06 m apart and with an outer diameter of 25 mm (SDR11). The pipes are connected in series, in a meandering pattern covering an area of approximately 4 m × 20 m and the flow rate is 12 L/min. The properties of the untreated material are listed in Table 1. The MICP treatment is applied to the subbase layer, composed of fine sand, which have been successfully treated using MICP (Xiao et al., 2022). Since subbase layer is directly next to the GHEs, enhancing the subbase's thermal conductivity improves heat transfer between the GHEs and the surrounding soil, thereby increasing the overall system performance. The MICP-treated location and the potential system heat transfer enhancements are shown in Figure 2.

Table 1. Material properties.

Material	Description	Density [kg/m^3]	Specific heat capacity [J/(kg·K)]	Thermal conductivity [W/(m·K)]	Thickness [m]
Asphalt	Road surface	2400	850	1.3	0.10
Gravel	Base	2200	944	1.4	0.20
Fine sand*	Subbase	1630	1185	0.3	0.20
Natural soil*	Subgrade	2100	840	0.9	10
Water	Carrier fluid	998	4158.5	0.58	-

*The range of thermal conductivity values used in the analysis are given in Table 2.

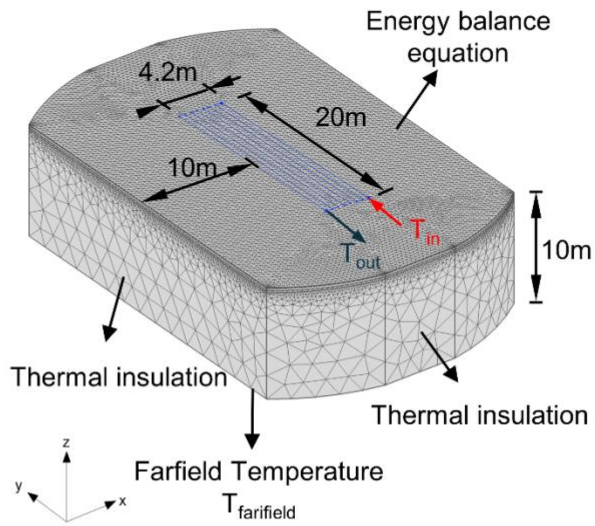

Figure 1. Meshed FE model with key boundary conditions.

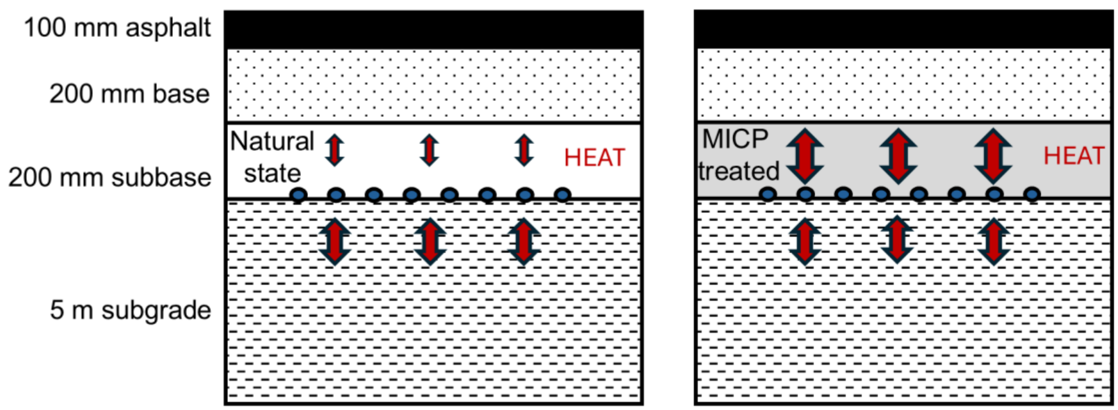

Figure 2. Cross-sectional comparison of a natural state pavement system (left) and an MICP-treated pavement system (right) (not to scale).

Simulation Inputs and Conditions.

This study evaluates the thermal performance and feasibility of MICP-treated geothermal pavements by varying key parameters. As illustrated in Figure 2, the MICP treatment is applied to the subbase layer, which consists of sandy soil. This treatment enhances the soil thermal properties and serves as a cushion for the GHEs located at the subgrade-subbase interface. Because the degree of saturation heavily influences the effectiveness of MICP in improving thermal performance, it is essential to account for seasonal variations in moisture content caused by changes in precipitation and temperature.

Experimental data collected by Martinez et al. (2019) is used as input to the simulations. Their results present the thermal conductivity of sandy soil treated with $CaCO_3$ contents ranging from 0 wt% to 4.1 wt% at different degrees of saturation. The sand soil used in their study was a poorly graded quartz sand (Ottawa 50-70 sand) with a mean particle diameter of 0.26 mm and a porosity of 0.38. The data from Martinez et al. (2019), replicated in Figure 3, show that the increase in thermal conductivity due to MICP treatment stabilises with high saturation levels, with only modest enhancement at saturation levels exceeding 30%. At these levels, heat transfer in soil is dominated by water, reducing the effectiveness of additional $CaCO_3$ grain-to-grain contacts. Therefore, this study examines MICP-treated soil thermal conductivity at 0%, 10%, and 30% saturation to capture the most relevant scenarios for evaluating its impact on thermal performance.

In the simulations, soil density and heat capacity are kept constant, focusing on variations in thermal conductivity as the key factor influencing heat transfer. A range of subgrade thermal conductivity values is considered to represent different soil conditions. Additionally, the possibility of a thin crust layer forming at the subgrade surface, due to low porosity, is represented by a 0.08 m high thermal conductivity layer. This simplification accounts for potential variability in MICP precipitation. Key variables considered in this study are summarised in Table 2.

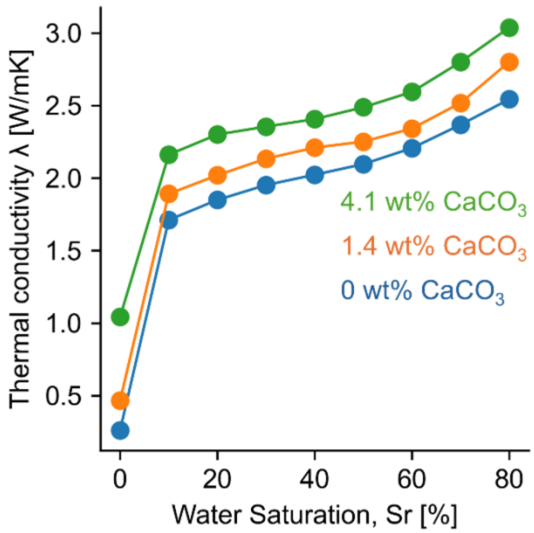

Figure 3. Thermal conductivity variation due to MICP treatment under different degrees of saturation for Ottawa 50-70 sand with a porosity of 0.38 (adapted from Martinez et al., 2019).

Table 2 Conditions Considered in this Study.

Variables	**Parameter values**
Subbase MICP treatment, [wt% $CaCO_3$]	0 (no treatment), 1.4, 4.1
Subbase degree of saturation, Sr [%]	0 (dry), 10, 30
Subbase thermal conductivity, $\lambda_{subbase}$ [W/(m·K)]	As shown in Figure 3
Subgrade thermal conductivity, $\lambda_{subgrade}$ [W/(m·K)]	0.3, 0.3*, 0.9, 1.6, 2.0

*Formation of a thin crust MICP layer at subgrade due to penetration of MICP solution

Thermal Load Distribution and Evaluation.

For the design life of a general GSHP system, the operating fluid temperature in the pipes should remain within a reasonable temperature range, typically between 0°C and 40°C, to ensure system functionality (Makasis et al., 2018). The thermal load, which defines the amount of energy that a GSHP system extracts from/rejects to the ground, is one of the key parameters that determines the operating fluid temperature. In this analysis, Adelaide, SA is selected as study location, which has a Mediterranean climate and experiences mild winters and warm, dry summers, resulting in a relatively balanced thermal demand profile. This balanced load case assists in assessing both heating and cooling potential in geothermal pavements. The weather and a typical residential thermal load profile in Adelaide are shown in Figure 4.

To evaluate the efficiency of MICP-treated geothermal pavements for Adelaide's conditions, the analysis focuses on the annual energy output per metre length of road (4.2 m width). This metric is determined by scaling the thermal demand, shown in Figure 4 (right), and assessing the resulting fluid temperatures, to ensure they remain within typical heat pump operating ranges.

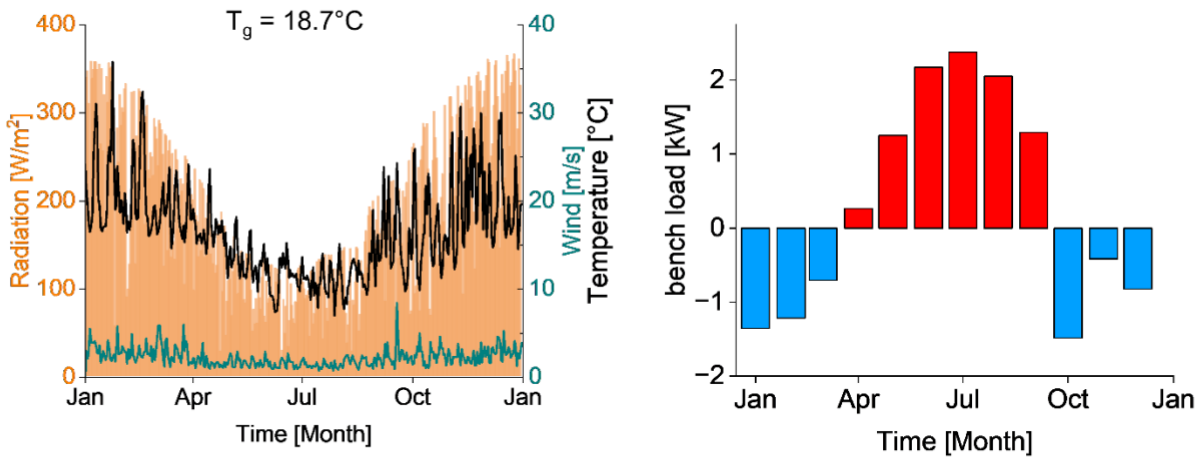

Figure 4. Adelaide weather data (left) and typical residential thermal load profile (right).

RESULTS AND DISCUSSION

Thermal performance of MICP-treated geothermal pavements.

The effect of the degree of saturation of the subbase on the effectiveness of MICP treatment is illustrated in the bar plot presented in Figure 5a. Results are presented for three $CaCO_3$ contents, 0 (untreated), 1.4, and 4.1 wt%, combined with three degrees of saturation, 0%, 10%, and 30%, all with a uniform subgrade thermal conductivity of 0.9 W/(m·K). The annual thermal energy output per metre road is used as an indicator of system performance.

As can be seen in Figure 5a, under dry road conditions (0% Sr), a noticeable increase in annual thermal energy supplied per metre road is observed with increasing $CaCO_3$ concentration. For example, for the designed subgrade conditions, a 4.1 wt% $CaCO_3$ content results in 32% additional thermal energy per metre road compared to the untreated cases. However, the impact of MICP treatment on the thermal behaviour of the system diminishes as degree of saturation increases. For a degree of saturation of 30%, the increase additional annual thermal energy supplied is marginal. This is because, at higher degrees of saturation, the water within the pores already enhances the conductive heat transfer by bridging the grains, and thus the additional grain-to-grain contacts generated through MICP only marginally increase the heat transport. In contrast, at low saturation levels, where the water phase is isolated and discontinuous, the thermal bridges built by $CaCO_3$ result in an appreciable thermal conductivity increase and, therefore, an overall thermal enhancement of the system.

In addition to the effects of degree of saturation, the impact of subgrade thermal conductivity ($\lambda_{subgrade}$) on system performance is explored. To isolate the effect of changes in $\lambda_{subgrade}$ on the effectiveness of MICP treatment of the subbase, a dry subbase is considered in this analysis. Results for this analysis are presented in Figure 5b, which shows the annual thermal energy output per metre road for subgrade thermal conductivity values ranging from 0.3 to 2.1

W/(m·K). Results indicate that increasing $\lambda_{subgrade}$ generally yields higher system output thermal energy. However, the relative benefits of MICP treatment diminish as $\lambda_{subgrade}$ increases. When the difference between $\lambda_{subgrade}$ and the subbase thermal conductivity is large, the subgrade becomes the primary heat transfer pathway, minimising the enhancement in thermal conductivity due to MICP in the subbase. For example, at a $\lambda_{subgrade}$ of 0.3 W/(m·K), a 4.1 wt% $CaCO_3$-treated subbase can deliver 80% more thermal load compared to the untreated case, whereas, at a higher $\lambda_{subgrade}$ of 2.1 W/(m·K), the additional thermal load from MICP treatment is less than 20%.

Moreover, because the GHEs are embedded at the interface of the subbase and subgrade, a scenario where an additional 0.08m MICP-treated layer is applied to the top of subgrade is considered for $\lambda_{subgrade}$ of 0.3 W/(m·K). As shown in Figure 5b, this additional superficial MICP treatment (left-most set of bars) further improves heat transfer around the GHEs, enhancing system performance by over 10% with a 4.1 wt% $CaCO_3$ treatment.

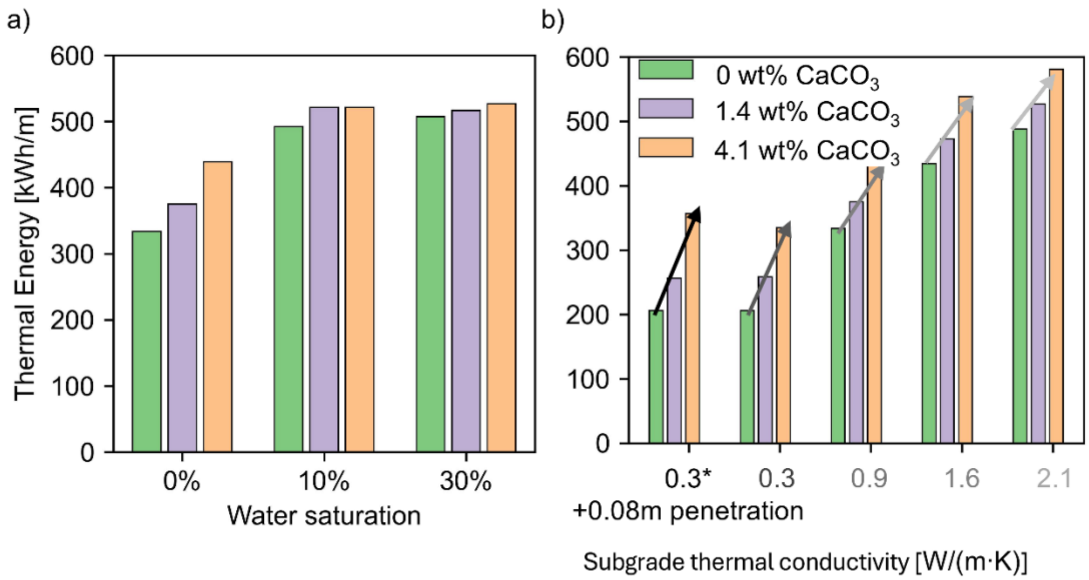

Figure 5. Annual thermal energy output/m road under: a) different levels of MICP treatment at different water saturation levels; b) different subgrade thermal conductivity (*Formation of a thin crust MICP layer at subgrade due to penetration of MICP solution).

Economic Performance of MICP-treated Geothermal Pavements.

While technical improvements are evident, economic feasibility remains a critical consideration for practical applications of MICP treatment within a geothermal context. This section evaluates potential costs and energy savings associated with MICP-enhanced geothermal pavements in Adelaide. The cost of MICP varies significantly based on cementation medium and bacterial growth conditions (Porter et al., 2021). In this study, the cost of producing $CaCO_3$ using ureolytic bacteria is estimated at 3.1 AUD/kg (Porter et al., 2021). The economic analysis compares the capital investment of MICP treatment with the additional thermal energy earnings it generates. The net present value of treatment (NPVT), representing the difference between capital investment and lifetime earnings from the extra energy provided, is calculated over a 25-year GSHP system lifespan. For this analysis, an electricity price of 0.28 AUD/kWh and a discount rate of 5% are used. The results are summarised in Figure 6.

As shown in Figure 6a, MICP-treated geothermal pavements are financially viable for Adelaide's climate and balanced load conditions when the subbase saturation level is below 10%. The highest NPVT (300 AUD) is achieved with a $\lambda_{subgrade}$ of 0.3 W/(m·K) under zero saturation, where MICP significantly boosts thermal output. As the value of $\lambda_{subgrade}$ increases, the benefit of MICP treatment reduces, leading to lower NPVT values. The analysis also examines the effect of adding a thin MICP-treated layer to the subgrade, which improves thermal efficiency by approximately 20%. This improvement results in a modest increase in NPVT, confirming both the technical and economic feasibility of the additional treatment layer.

To assess the sensitivity of NPVT to economic factors, a tornado analysis is shown in Figure 6b, focusing on MICP material cost, electricity cost, and discount rate. The plot shows that MICP material costs have the greatest influence on NPVT, with variations ranging from -100 AUD/m to 200 AUD/m. Lower MICP costs result in higher NPVT, indicating better economic performance. Changes in the discount rate, which reflects the time value of money and represents the rate at which future cash flows are discounted to present value, also affect NPVT. A lower discount rate increases the present value of future savings, while a higher discount rate decreases it. Electricity cost has less impact, with higher costs translating into greater energy savings.

Overall, the analysis shows that, while MICP can enhance geothermal system performance, its economic viability depends heavily on material costs, with potential benefits maximised in low-cost scenarios.

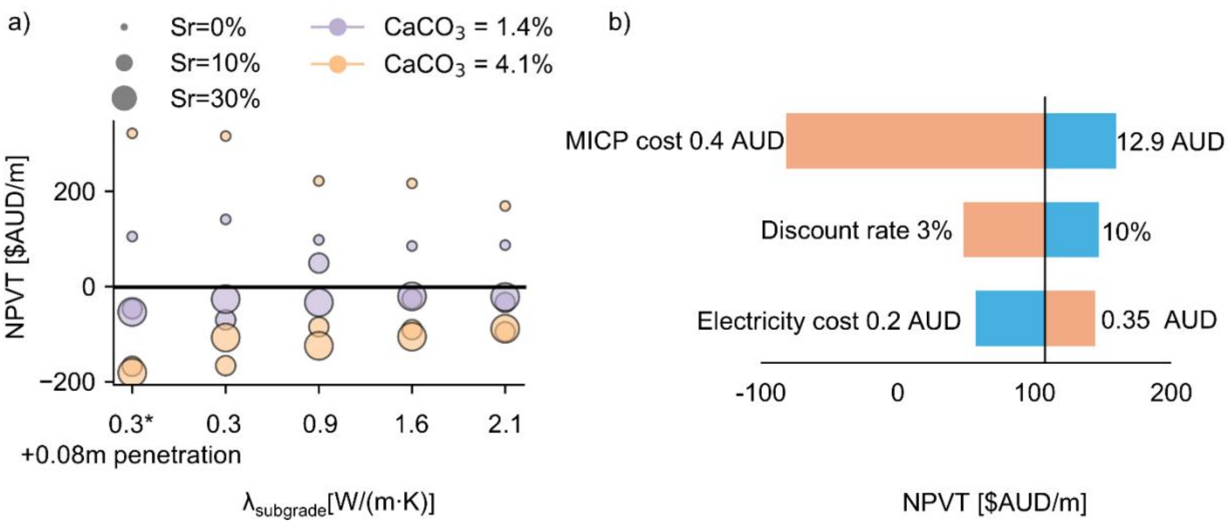

Figure 6. (a) Net present value of treatment (NPVT) for MICP-treated pavements under various saturation and $CaCO_3$ content conditions; (b) sensitivity of NPVT to key economic parameters.

CONCLUSION

This study evaluates the thermal and economic feasibility of incorporating microbial induced calcium carbonate precipitation (MICP) into geothermal pavements using a validated finite element model focused on Adelaide, South Australia. Results indicate that MICP treatment can significantly enhance geothermal system performance in dry subbase conditions, particularly when the subgrade thermal conductivity is low (<0.3 W/(m·K)), with increases in thermal energy provided of up to 80%. However, as subbase saturation increases beyond 10% or the subgrade thermal conductivity is much higher than that of the subbase layer, the benefits of MICP diminish.

Although higher $CaCO_3$ content can result in thermal advantages for all conditions, the applicability of the approach needs to be determined through its economic viability. The results of this study show that the feasibility of MICP is heavily influenced by the cost of treatment materials, with lower material costs leading to a more favourable net present value of treatment. At an MICP cost of 3 AUD/kg, NPVT is only positive when the subbase saturation level is below 10%, meaning that in these cases the economic benefits of the additional thermal energy yield outweigh the cost of treatment with MICP. A sensitivity analysis further highlights the influence of discount rate and electricity cost in determining economic outcomes, albeit at a lesser degree compared to the cost of treatment materials. Future studies will investigate extreme climates with heating- and cooling-dominant thermal load profiles, where harsher thermal gradients may influence the benefits and economic feasibility of MICP-treated pavements. Achieving uniform $CaCO_3$ precipitation in the subbase is critical for consistent thermal conductivity improvements, as variability could compromise system performance. Future models addressing this variability will provide deeper insights into the real-world applicability of MICP-treated geothermal pavements.

ACKNOWLEDGEMENTS

Funding from the Australian Research Council (ARC) (project number LP200100052) and the University of Melbourne is much appreciated. The second author would also like to acknowledge the support of the National Science Foundation (NSF) (Award No. 2343577).

REFERENCES

Arulrajah, A., Ghorbani, B., Narsilio, G., Horpibulsuk, S. & Leong, M. 2021. Thermal performance of geothermal pavements constructed with demolition wastes. *Geomechanics for Energy and the Environment*.

Clarà Saracho, A., Haigh, S. K. & Ehsan Jorat, M. 2021. Flume study on the effects of microbial induced calcium carbonate precipitation (MICP) on the erosional behaviour of fine sand. *Géotechnique,* **71,** 1135-1149.

DeJong, J. T., Mortensen, B. M., Martinez, B. C. & Nelson, D. C. 2010. Bio-mediated soil improvement. *Ecological Engineering,* **36,** 197-210.

del-Castillo-García, G., Borinaga-Treviño, R., Sañudo-Fontaneda, L. A. & Pascual-Muñoz, P. 2013. Influence of pervious pavement systems on heat dissipation from a horizontal geothermal system. *European Journal of Environmental and Civil Engineering,* **17,** 956-967.

Di Sipio, E. & Bertermann, D. 2017. Factors Influencing the Thermal Efficiency of Horizontal Ground Heat Exchangers. *Energies,* **10**.

Fu, T. & Haigh, S. K. 2024. Biocementation of a Well-Graded Gravelly Soil and Macromechanical Characterization. *Journal of Geotechnical and Geoenvironmental Engineering,* **150**.

Gu, X., Makasis, N., Motamedi, Y., Narsilio, G. A., Arulrajah, A. & Horpibulsuk, S. 2021. Geothermal pavements: field observations, numerical modelling and long-term performance. *Géotechnique***,** 1-48.

Insana, A. & Barla, M. 2020. Experimental and numerical investigations on the energy performance of a thermo-active tunnel. *Renewable Energy,* **152,** 781-792.

Kavanaugh, S. P. 2000. Field tests for ground thermal properties--methods and impact on ground-source heat pump design. Univ. of Alabama, Tuscaloosa, AL (US).

Khosravi, M., Phillips, A., Dorian, H., Durojaye, O., Cunningham, A., Gupta, M. & Parushev, E. 2024. Large-Scale Bio-Cementation Test to Improve Sub-Structures of Existing Asphalt and Concrete Roadways. *Geo-Congress 2024.*

Li, S., Wang, Y.-n., Liu, D., Garg, A. & Lin, P. 2020. Exploring an environmentally friendly Microbially Induced Calcite Precipitation (MICP) technology for improving engineering properties of cement-stabilized granite residual soil. *Nature Environment and Pollution Technology,* **19,** 1211-1218.

Makasis, N. & Narsilio, G. A. 2020. Energy diaphragm wall thermal design: The effects of pipe configuration and spacing. *Renewable Energy,* **154,** 476-487.

Makasis, N., Narsilio, G. A., Bidarmaghz, A. & Johnston, I. W. 2018. Ground-source heat pump systems: The effect of variable pipe separation in ground heat exchangers. *Computers and Geotechnics,* **100,** 97-109.

Martinez, A., Huang, L. & Gomez, M. G. 2019. Thermal conductivity of MICP-treated sands at varying degrees of saturation. *Géotechnique Letters,* **9,** 15-21.

Motamedi, Y., Makasis, N., Gu, X., Narsilio, G. A., Arulrajah, A. & Horpibulsuk, S. 2021. Investigating the thermal behaviour of geothermal pavements using Thermal Response Test (TRT). *Transportation Geotechnics,* **29**.

Mujah, D., Shahin, M. A. & Cheng, L. 2016. State-of-the-Art Review of Biocementation by Microbially Induced Calcite Precipitation (MICP) for Soil Stabilization. *Geomicrobiology Journal,* **34,** 524-537.

Porter, H., Mukherjee, A., Tuladhar, R. & Dhami, N. K. 2021. Life Cycle Assessment of Biocement: An Emerging Sustainable Solution? *Sustainability,* **13**.

Portugal, C. R. M. e., Fonyo, C., Machado, C. C., Meganck, R. & Jarvis, T. 2020. Microbiologically Induced Calcite Precipitation biocementation, green alternative for roads – is this the breakthrough? A critical review. *Journal of Cleaner Production,* **262**.

Rahman, M. M., Hora, R. N., Ahenkorah, I., Beecham, S., Karim, M. R. & Iqbal, A. 2020. State-of-the-Art Review of Microbial-Induced Calcite Precipitation and Its Sustainability in Engineering Applications. *Sustainability,* **12,** 6281.

Van Paassen, L. A. 2009. Biogrout, ground improvement by microbial induced carbonate precipitation.

Venuleo, S., Laloui, L., Terzis, D., Hueckel, T. & Hassan, M. 2016. Microbially induced calcite precipitation effect on soil thermal conductivity. *Géotechnique Letters,* **6,** 39-44.

Wang, Z., Zhang, N., Ding, J., Li, Q. & Xu, J. 2020. Thermal conductivity of sands treated with microbially induced calcite precipitation (MICP) and model prediction. *International Journal of Heat and Mass Transfer,* **147**.

Xiao, Y., Tang, Y., Ma, G., McCartney, J. S. & Chu, J. 2021. Thermal Conductivity of Biocemented Graded Sands. *Journal of Geotechnical and Geoenvironmental Engineering,* **147**.

Xiao, Y., Xiao, W., Ma, G., He, X., Wu, H. & Shi, J. 2022. Mechanical Performance of Biotreated Sandy Road Bases. *Journal of Performance of Constructed Facilities,* **36**.

Zeinali, S., Rizvi, Z. & Wuttke, F. 2023. Thermal conductivity of dried biocemented sand at higher calcification. *Symposium on Energy Geotechnics 2023***,** 1 - 2.

Zhang, K., Tang, C. S., Jiang, N. J., Pan, X. H., Liu, B., Wang, Y. J. & Shi, B. 2023. Microbial-induced carbonate precipitation (MICP) technology: a review on the fundamentals and engineering applications. *Environ Earth Sci,* **82,** 229.

Zhong, Y., Narsilio, G. A., Makasis, N. & Scott, C. 2022. Experimental and numerical studies on an energy piled wall: The effect of thermally activated pile spacing. *Geomechanics for Energy and the Environment,* **29**.